# INVESTIGATION OF MEMBRANE ACTION IN MODEL SCALE SLABS SUBJECT TO HIGH TEMPERATURES

S. J. Foster[1], I. W. Burgess[1] and R.Plank[2]

[1] Department of Civil & Structural Engineering, University of Sheffield, Sheffield, S1 3JD, UK; Emails: s.j.foster@sheffield.ac.uk, ian.burgess@sheffield.ac.uk

[2] School of Architectural Studies, University of Sheffield, S10 2TN, UK; Email: r.j.plank@sheffield.ac.uk

## ABSTRACT

Full-scale fire tests in the multi-storey steel framed building at Cardington have shown that the composite floor system, even with unprotected steel downstand beams, does not collapse, even at very large deformations. This enhanced resistance is attributed to tensile membrane forces which assist in maintaining the structural integrity through diaphragm action.

The Building Research Establishment in the UK has developed a new design method for composite floors in fire, based on a simplified model of the membrane action of rectangular slabs. This paper presents the results from tests on a number of loaded horizontally unrestrained small-scale slabs at elevated temperatures. The main purpose of these tests was to investigate the influence of thermal curvature on the failure mechanisms of rectangular slabs. The more detailed issues being studied include the effects of reinforcement percentage and reinforcement bond strength at high temperatures on the final integrity failure due to tensile cracking. The small-scale slab tests have also been modelled using the University of Sheffield's in-house software, *Vulcan*.

Observations from the high-temperature tests have shown that the mechanism of failure may differ from that assumed in the simplified design method. The results from the numerical modelling have been compared with both experimental and the simplified method and show good agreement.

## KEYWORDS

Tensile membrane action, composite floors, concrete, slabs, large displacements, high temperature experiments, fire performance.

## INTRODUCTION

During 1995 and 1996, six localised fire tests (British Steel Swinden technology Centre, 1999) were conducted on the full-scale, eight storey, steel-framed building at the Building Research Establishment's Cardington Laboratory. These tests showed that composite floor slabs with unprotected steel downstand beams have large reserves of fire resistance beyond that predicted by conventional design methods. The enhanced fire resistance was attributed to in-plane forces which assist in carrying the loading though diaphragm (or tensile membrane) action. A simplified design method (Bailey, 2000) was subsequently developed using a simplified model of tensile membrane action, which was a significant improvement on previous design methods based on flexural behaviour. By incorporating this enhancement to the resistance of the composite floor slab, it is often possible for a significant number of steel beams within a given floor space to be left unprotected.

This simplified design method was initially limited in scope to isotropic slabs; those for which the total area of reinforcement is equal in both the short and long span directions. This has recently been extended to incorporate orthotropic arrangements of reinforcement (Bailey, 2003 and Foster *et al.*, 2004). A series of experiments was conducted by the authors on horizontally unrestrained concrete slabs, with both isotropic and orthotropic reinforcement. The influence of bond was investigated by comparing the results from slabs using smooth and deformed (ribbed) reinforcement. These slabs were tested at ambient temperature to verify the assumptions made in the simplified design method. However, it can not be assumed that the basic behaviour observed at ambient temperature will necessarily remain the same at elevated temperatures. The test series has recently been extended to the use of elevated temperatures, in order to further investigate the mechanics of the membrane action and to provide comparisons with the simple design method. This paper presents the results from the experiments on horizontally unrestrained rectangular and square concrete slabs with varying percentages of isotropic reinforcement, at elevated temperatures. The influence of bond between the reinforcing wires and concrete at elevated temperature is considered by comparing the results from slabs using smooth and deformed (ribbed) reinforcing wires.

## SIMPLIFIED DESIGN METHOD

The simplified design method assumes a mode of failure that was previously observed in many ambient-temperature tests, mainly conducted on flat, isotropically reinforced slabs, whose cracking pattern is illustrated in Figure. 1.

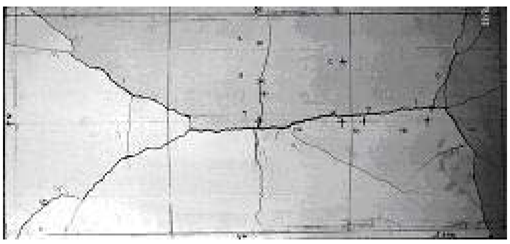

Figure 1: Cracking pattern observed in slabs due to tensile membrane action at ambient temperature.

The typical mode of failure in these tests, following tensile membrane action, was the formation of a full-depth localised crack across the shorter span of the slab. The full derivation of the simple design method for isotropic and orthotropic reinforcement has been published elsewhere (Bailey, 2003) and will not be repeated here.

## NUMERICAL MODELLING

Numerical studies have been undertaken using the University of Sheffield software *Vulcan* (Huang, 2003a). Three-dimensional numerical models have been created of the model-scale slabs. The concrete elements used were quadrilateral 9-noded shell elements. The slab elements were sub-divided into 10 layers of which 8 represent the concrete and two the steel reinforcement. The recorded temperatures through the depth of the slab have been used to calculate the temperature history for each layer. The reinforcing steel bars were modelled using a smeared approach, the thickness of each reinforcement layer being set so that its cross-sectional area was equal to the total cross-sectional area of slab reinforcement in the direction of the layer of bars represented; the layer's constitutive properties were set as uniaxial. Perfect bond was assumed between the reinforcing steel layers and the surrounding concrete. The Eurocode 4 Part 1.2 (2003) concrete material properties were used, together with the concrete strengths measured on the day of the test and the yield strength of the reinforcing wire.

## TEST CONFIGURATION AND INSTRUMENTATION

Four slab sizes were tested, of nominal dimensions (in mm) 920x620x15, 920x620x22, 600x600x15, and 600x600x22 with the supported areas being 850x550 and 550x550 respectively. The actual depth of the slab varied slightly between tests, and measurements were made after each test (Tables 1, 2 and 3, in the Appendix). The test setup in these experiments was very similar to the previous tests at ambient temperature (Foster *et al.*, 2004). The slabs were tested in a loading rig in which equal constant concentrated loads were maintained at 12 points for the rectangular slabs and 4 points for the square slabs (Figure. 2).

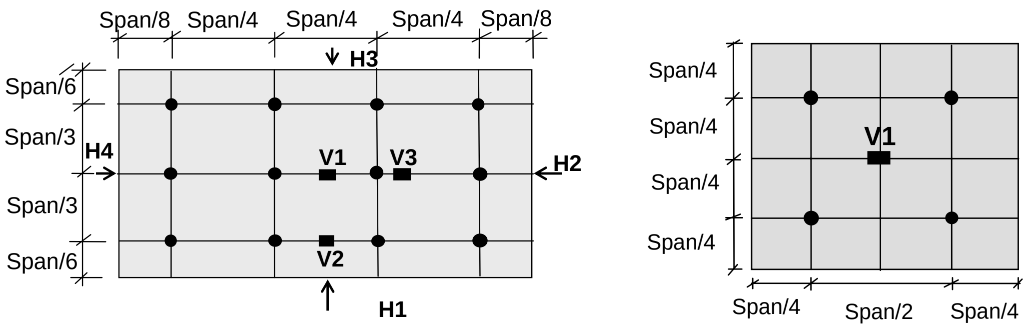


(a) (b)

Figure 2: Location of load and displacement gauges for (a) rectangular and (b) square slabs

The loading frame and test set-up is shown in Figure. 3; the supporting frame was adjustable to allow the testing of the square slabs. The applied load remained vertical with the aid of ball-joints which allowed the loading system to rotate as the slab deflected. The slab was placed on a supporting frame, providing vertical support around the perimeter. The heating was generated by four electrical elements contained within an insulated steel box (Figure. 3).

The slabs were reinforced with 0.71mm diameter smooth or deformed steel wire; distributed isotropically. The deformed wire was fabricated by indenting the smooth wire using a purpose-built machine. The percentage of reinforcement in any slab cross-section varied between 0.05% and 0.25%. The measured yield strengths of reinforcement and the compressive strengths of concrete are shown in Tables 1, 2 and 3 in the Appendix. The temperatures of the lower surface, the reinforcement level, and the upper surface of the slab were measured using 12 thermocouples placed at key locations.

Figure 3: Typical arrangement of test set-up and supporting frame

## RESULTS

### *Observations of slab behaviour*

The slabs were subjected to the constant imposed load before the heating elements were switched on; the values of load are contained in Tables 1, 2 and 3 in the Appendix. The rectangular and square slabs behaved similarly; approximately 10-15 minutes after the furnace was switched on, diagonal cracking occurred across the corners as the slab deflected into double curvature. After 20 minutes, a single transverse crack could be seen forming on the upper surface of the slab in its central region (Figure. 4). Over time, this crack developed outwards in the transverse short-span direction towards the long edges of the slab. Most of the slabs developed crack patterns resembling a yield line mechanism towards the end of the test, usually after about 2 hours. The crack patterns resembled those of similar slabs tested at ambient temperature (Foster *et al.*, 2004), except that the diagonal yield lines tended to align more in the long direction of the slab (Figure. 4(c)), giving a much shorter central yield line than usual. The formation of these yield lines seems to depend on the applied load level, while the development of the initial transverse crack after the slab has deflected into double curvature appears to be associated with its thermal bowing.

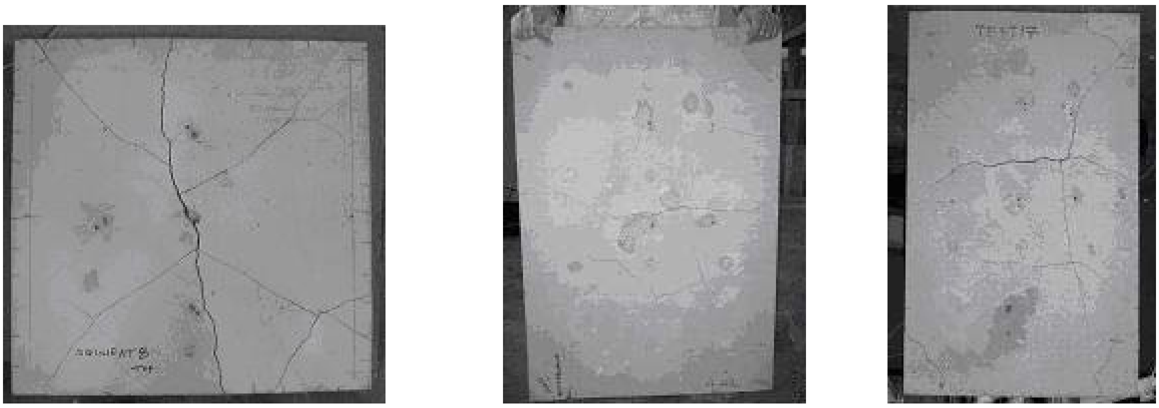

(a) (b) (c)

Figure 4: View of slab upper surface after test, a) 550x550mm Test 7, b) 850x550mm Test 15, (c) 850x550 Test 17

It was apparent that, for Tests 12, 14, and 17, on slabs reinforced with deformed wire, once the major tension crack had formed across the short span the reinforcement across the crack fractured. For the slabs reinforced with smooth wire, for example Test 15 (Figure 4(b)), the transverse crack re-closed after the test, and the reinforcement had not fractured. The slabs reinforced with deformed wire achieved a stronger bond between the concrete and steel and the straining of the reinforcement occurred over a smaller free length, leading to fracture strains happening at quite small crack widths.

***Deflections***

The mid-span vertical deflections of the slabs tested are shown in Figures 5, 6 and 7. Some of these tests attained deflections up to *Span/12*. All the slabs showed similar rates of deflection between 20°C and 150°C. The slabs of depth 22mm with reinforcement placed 7.5mm from the bottom surface (Tests 9, 10, 11, 20 and 21) had deflections lower than those of the 15mm thick slabs (Figure 7). The rate of deflection for slabs reinforced with smooth wire (Tests 15 and 13) can be seen to be less than those for the equivalent slabs using deformed wire (Tests 17 and 12), as shown in Figure. 6.

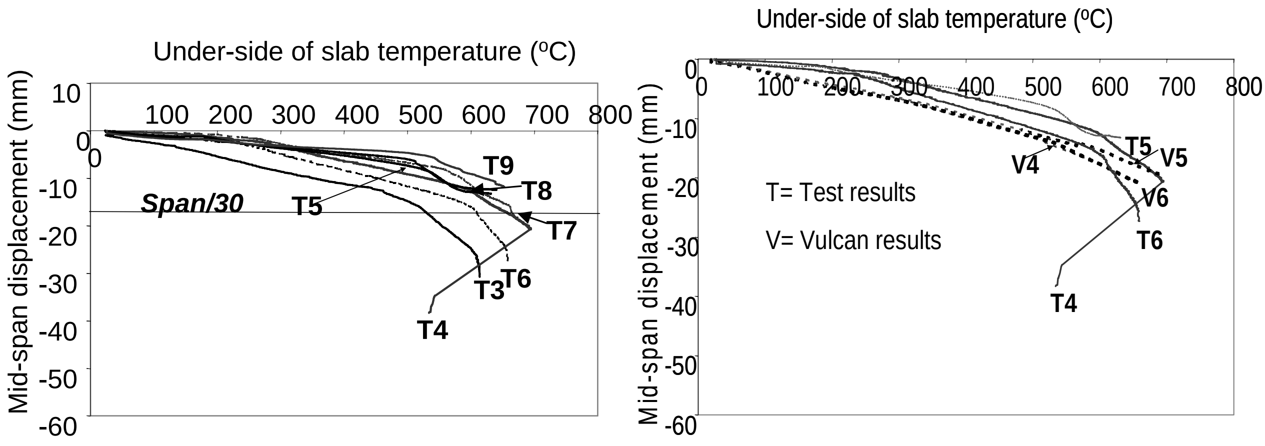


Figure 5: Vertical Displacements of 600x600x15mm square slabs

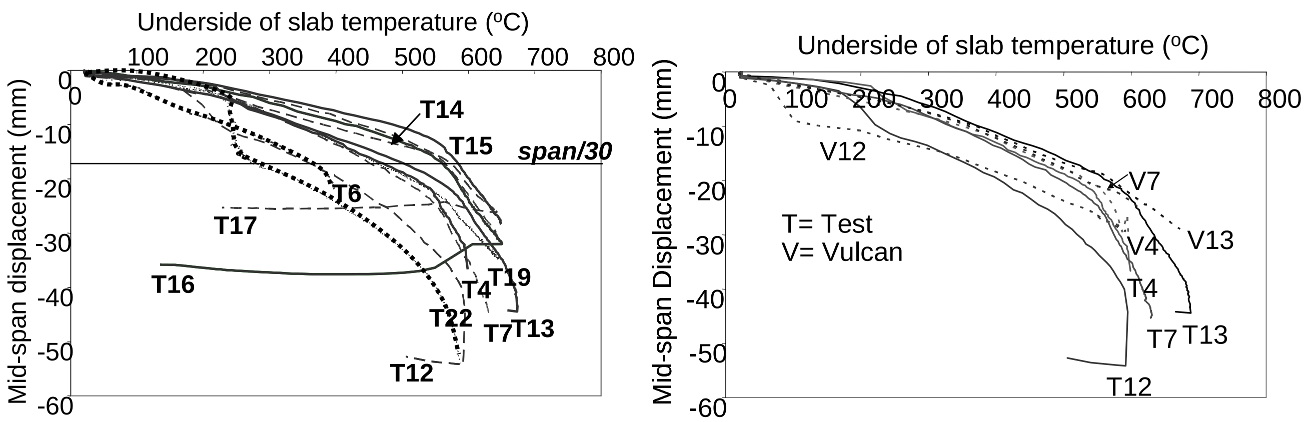


Figure 6: Vertical displacements of 920x620x15mm rectangular slabs

The square slabs performed similarly to the rectangular ones in the range 20-220°C, and performed better above this temperature range (Figure 5). The square slabs of depth 24mm (Tests 8 and 9) had lower deflections at any given temperature compared with those for slabs of depth 15mm. On comparing the percentages of reinforcement for both the rectangular and square slabs, the results show that the slabs with lower percentages of reinforcement reach lower deflections towards the latter stages of the test than slabs reinforced with higher percentages (Figures 5 and 6).

Numerical modelling studies have been carried out using *Vulcan*, and comparisons are presented in Figures 5, 6 and 7. Mesh studies were undertaken at ambient temperature in order to validate the model. The results show good correlation between test and numerical results for both the square and rectangular slabs. This seems to indicate that, even though the numerical model does not consider the effects of bond strength on reinforcement fracture, it predicts behaviour very similar to that shown in the tests.

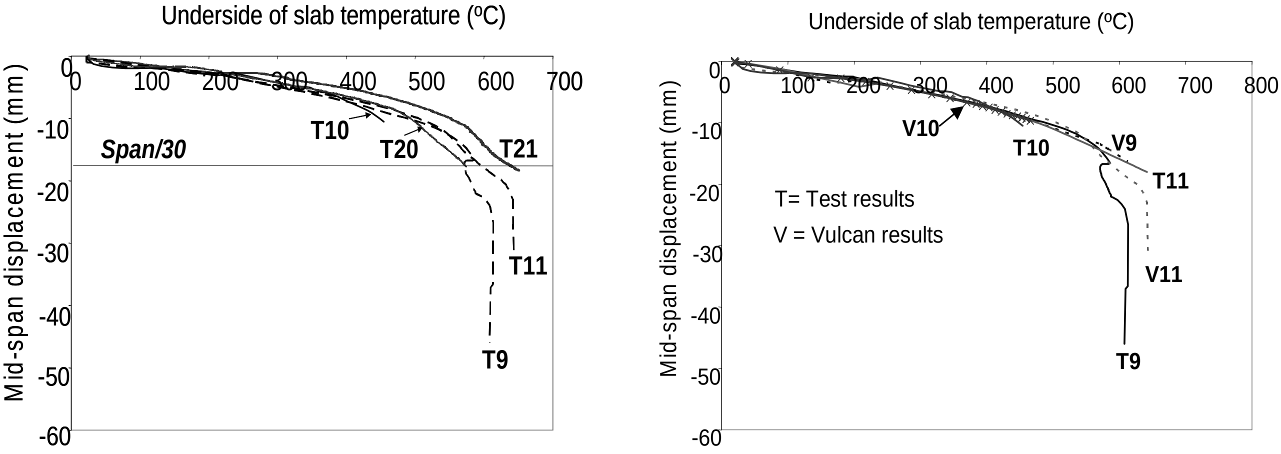


Figure 7: Vertical displacements of 920x620x22mm rectangular slabs

A reduced, high-temperature yield-line load capacity can be calculated using the reduced strengths of the reinforcing steel at elevated temperatures. The experimentally measured steel temperatures were used to assign appropriate strength reduction factors from Eurocode 3 Part 1.2 (2003). Figure 8 plots the enhanced load ratios carried by the slabs in some of the tests in terms of the reduced yield-line capacities, showing that the slabs carried loads far greater than yield line predictions. In both sets of tests for the rectangular and square slabs, the lightly reinforced slabs showed a greater rise in enhancement than the more highly reinforced slabs. The square slabs also achieved higher enhancements than the corresponding rectangular slabs. For the rectangular slabs, at displacements greater than 15mm this capacity was demonstrably enhanced by tensile membrane action, whereas for the square slabs this occurred from a lower deflection of 7mm.

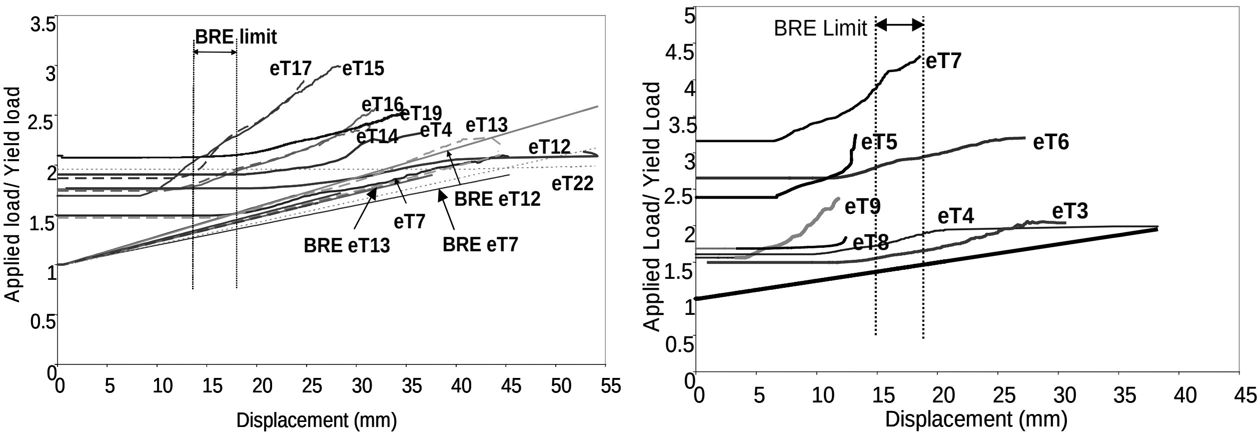


(a) (b)

Figure 8: Enhancement factors for a) rectangular slabs and b) square slabs

On comparing the behaviour of slabs reinforced with smooth wire with that of those reinforced with deformed wire, it can be seen that there is no significant difference between the enhancements at low deflections, but depending on the slab failure the enhancements greatly increase.

## CONCLUSIONS

This paper presents the main results from a number of loaded high-temperature tests conducted on horizontally unrestrained slabs. An electrical heating system and self-supporting frame have been developed to enable the slabs to be heated up to lower-surface temperatures of about 700°C. Both the rectangular and square slabs have in general performed very well, with enhancements of up to 4.5 times the initial yield-line capacity achieved. This enhanced resistance is attributed to membrane forces, which assist in maintaining the structural integrity through diaphragm action.

A major purpose of these tests was to investigate the influence of thermal curvature on the failure mechanisms of rectangular slabs. Observations from the high-temperature tests have shown that the cracking mechanism differs in some respects from that observed at ambient temperature. At ambient temperature, four flat facets of the slab rotate about the edge supports and yield line cracks are formed as a low-deflection mechanism which is forced into membrane action at high deflections. At high temperatures, the slab initially deflects into double curvature, generating full-depth cracking across its short span, and may later form a less distinctive yield line mechanism. The comparisons between the numerical model *Vulcan* and the experiments have shown that *Vulcan* predicts deflections accurately, even though it does not model discrete cracking.

## ACKNOWLEDGMENT

*The authors gratefully acknowledge sponsorship of the first author by the Engineering and Physical Sciences Research Council of the United Kingdom, and by Arup Fire Ltd.*

## REFERENCES

Bailey, C.G., (2000) *Design of steel structures with composite slabs at the fire limit state*. BRE Final Report to the Department of the Environment, Transport and Regions, Building Research Establishment, Garston, UK.

Bailey, C.G., (2003) ’Efficient arrangement of reinforcement for membrane behaviour of composite floor slabs in fire conditions’. *J. Construct. Steel Research*, **59**, pp931-949

British Steel Swinden Technology Centre, (1999**)** *The behaviour of multi-storey framed buildings in fire: a European joint research programme,* British Steel Swinden Technology Centre.

Eurocode 4, (2003) *Design of composite steel and concrete structures: Part 1.2: Structural rules, Structural fire design, prEN 1994-1-2*. European Committee for Standardisation.

Eurocode 3, (2003) *Design of steel structures: Part 1.2: General rules, Structural fire design, prEN 1993-1-2*. European Committee for Standardisation.

Foster, S.J., Bailey, C.G., Burgess, I.W. and Plank, R.J., (2004) 'Experimental Behaviour of Concrete Floor Slabs at Large Displacements', *Engineering Structures,* **26** (9), (2004) pp 1231-1247.

Huang, Z, Burgess, I.W. and Plank R.J., (2003) ’Modelling membrane action of concrete slabs in composite buildings in fire: Part I: Theoretical development’. *Journal of Structural Engineering*, ASCE, **129** (8), (2003) pp1093-1102.

Huang, Z, Burgess, I.W. and Plank R.J., (2003) ’Modelling membrane action f concrete slabs in composite buildings in fire: Part II: Validations. *Journal of Structural Engineering*, ASCE, **129** (8), (2003) pp1103-1112.

| Test | Reinf. Area (%) | t (mm) | Bar Type | fc ($N/mm^2$) | Yield Line Capacity Wu ($kN/m^2$) | Imposed Load Q ($kN/m^2$) | Load Ratio Q/Wu |
|---|---|---|---|---|---|---|---|
| 4 | 0.15 | 17 | S | 37 | 2.34 | 4.46 | 1.9 |
| 5 | 0.15 | 13 | D | 40 | 1.58 | 4.58 | 2.9 |
| 7 | 0.15 | 17 | D | 40 | 2.21 | 3.30 | 1.5 |
| 6 | 0.05 | 17 | S | 44 | 0.94 | 2.67 | 2.8 |
| 15 | 0.05 | 16 | S | 40 | 0.89 | 1.50 | 1.7 |
| 17 | 0.05 | 17 | D | 39 | 0.89 | 1.66 | 1.87 |
| 12 | 0.25 | 14.6 | D | 38 | 3.62 | 6.4 | 1.77 |
| 13 | 0.25 | 16 | S | 38 | 4.63 | 6.8 | 1.47 |
| 22 | 0.25 | 17 | S | 40 | 4.94 | 9.60 | 1.94 |
| 14 | 0.1 | 16.8 | D | 40 | 1.47 | 2.54 | 1.73 |
| 16 | 0.1 | 17 | S | 38 | 1.57 | 2.76 | 1.76 |
| 19 | 0.1 | 17 | S | 37.5 | 2.34 | 4.90 | 2.09 |
| 18 | 0.1 | 24 | S | 37.1 | 4.60 | 4.87 | 1.06 |

**TABLE 1**
Slab 920x620x15mm, reinforcement placed at half depth of slab
S=Smooth wire; D= Deformed wire

| Test | Reinf. Area (%) | t (mm) | Bar Type | fc ($N/mm^2$) | Yield Line Capacity Wu ($kN/m^2$) | Imposed Load Q ($kN/m^2$) | Load Ratio Q/Wu |
|---|---|---|---|---|---|---|---|
| 9 | 0.1 | 23 | D | 42 | 4.32 | 6.39 | 1.48 |
| 20 | 0.1 | 26 | S | 40 | 5.17 | 7.1 | 1.37 |
| 10 | 0.05 | 24 | D | 39 | 2.49 | 4.7 | 1.89 |
| 11 | 0.05 | 23 | S | 39 | 2.48 | 5.92 | 2.39 |
| 21 | 0.05 | 26 | D | 40 | 2.79 | 4.42 | 1.58 |

**TABLE 2**
920x620x22mm, reinforcement placed at 7.5mm from bottom of slab.

| Test | Reinf. Area (%) | t (mm) | Bar Type | fc ($N/mm^2$) | Yield Line Capacity Wu ($kN/m^2$) | Imposed Load Q ($kN/m^2$) | Load Ratio Q/Wu |
|---|---|---|---|---|---|---|---|
| 3 | 0.25 | 15 | S | 38 | 5.95 | 8.90 | 1.50 |
| 4 | 0.15 | 15.1 | D | 40 | 2.87 | 4.61 | 1.61 |
| 5 | 0.05 | 15.1 | D | 39 | 1.16 | 2.76 | 2.38 |
| 6 | 0.1 | 15 | S | 38 | 2.04 | 5.40 | 2.65 |
| 7 | 0.05 | 15 | S | 40 | 1.23 | 3.87 | 3.15 |
| 600x600x22mm, reinforcement placed at 7.5mm from bottom of slab | | | | | | | |
| 8 | 0.05 | 24 | D | 39 | 3.62 | 6.10 | 1.69 |
| 9 | 0.05 | 24 | S | 39 | 3.83 | 6.00 | 1.57 |

**TABLE 3**
600x600x15mm, reinforcement placed at half depth of slab